

High-extinction-ratio micro polarizing beam splitter for short wavelength optical storage applications

Chi-Hung Lee

Department of Photonics & Institute of Electro-Optical Engineering,
National Chiao Tung University, Hsin-Chu 300, Taiwan
tainanncku@hotmail.com

Yi Chiu

Department of Electrical and Control Engineering,
National Chiao Tung University, Hsin-Chu 300, Taiwan
yichiu@mail.nctu.edu.tw

Han-Ping D. Shieh

Department of Photonics & Display Institute
National Chiao Tung University, Hsin-Chu 300, Taiwan

Abstract: A surface-micromachined high-extinction-ratio polarizing beam splitter (PBS) using low absorptive silicon nitride layers for blue wavelength applications are demonstrated. The micro polarizing beam splitter consists of novel stack of two silicon nitride layers separated by an air gap. A PBS optimization model is established to achieve both high extinction-ratio and adequate process margin. The polarization extinction ratios of 25 dB for the reflected light and 15 dB for the transmitted light were experimentally achieved at $\lambda=405$ nm. The fabrication of the PBS is compatible with other micro diffractive elements to build a micro optical bench, thus, feasible for short wavelength optical storage applications.

©2005 Optical Society of America

OCIS codes: (230.5440) Polarization-sensitive devices; (310.6860) Thin films, optical properties; (350.3950) Micro-optics; (220.4000) Microstructure fabrication; (210.0210) Optical data storage; (999.9999) Short Wavelength.

References and links

1. C. Pu, Z. Zhu, and Y. H. Lo, "Surface micromachined integrated optical polarization beam splitter," *IEEE Photon. Technol. Lett.* **10**, 988-990 (1998).
2. K. K. Schuegraf, ed, *Thin Film Deposition Process and Techniques* (Noyes Publications, Park Ridge, NJ 1988).
3. S. Wolf and R. Tauber, *Silicon Processing for the VLSI Era, Vol. 1: Process Technology* (Lattice, Sunset Beach, CA, 1986).
4. M. Sekimoto, H. Yoshihara, and T. Ohkubo, "Silicon nitride single-layer x-ray mask," *J. Vac. Sci. Technol.* **21**, 1017-1021 (1982).
5. J. G. E. Gardeniers, H. A. C. Tilmans and C. C. G. Visser, "LPCVD silicon-rich silicon nitride films for applications in micromechanics, studied with statistical experimental design," *J. Vac. Sci. Technol. A*, **14**, 2879-2892 (1996).
6. D. Maier-Schneider, A. Ersoy, J. Maibach, D. Schneider, and E. Obermeier, "Influence of annealing on elastic properties of LPCVD silicon nitride and LPCVD polysilicon," *Sens. Materials* **7**, 121-129 (1995).
7. M. Born and E. Wolf, *Principles of Optics* (University Press, Cambridge, 1999), Chap. 1.

1. Introduction

High-extinction-ratio micro polarizing beam splitters (micro PBS) are required in micro optical systems for sensing and signal processing when the polarization state is a concern. For example, in an optical storage system, a high-extinction-ratio micro PBS is required to divide the incident light into a highly reflected TE mode and a highly transmitted TM mode to reduce the optical noise. The reflected TE mode is used to monitor the light intensity; the TM mode is used to read and write the data on the disk. A surface micromachined poly-silicon PBS was first proposed by Pu *et al.* and demonstrated to operate well for near IR [1]. For short wavelength applications, such as 405nm for blue light storage system, the poly-silicon based PBS is not suitable due to its high absorption. Among the materials used in polysilicon based surface micromachining, silicon nitride and silicon dioxide have high transparency in the visible spectrum range. However, silicon dioxide is usually used as the sacrificial layer. Therefore, silicon nitride was investigated as the optical material.

Employing the polarization sensitive characteristic of the dielectric film, a silicon nitride film at the Brewster angle incidence can serve as a PBS. To achieve higher polarization extinction ratio, multilayer coating on the PBS surface or cascading several PBS's in tandem are required. The former method is limited by the materials available in surface micromachining, while the latter requires large area and operates only for the transmitted waves. To overcome the constraints of available materials and die size, a SiN/Air/SiN stack operating at the Brewster angle incidence is first proposed to replace the conventional multilayer coating. The stack is composed of two silicon nitride layers (as high-refractive-index layers) separated by an air gap (as a low-refractive-index layer). At the Brewster angle incidence, the reflectivity of the TM mode will be nominally zero. By choosing specific thicknesses of the silicon nitride layers and the air gap, the reflectivity of the TE mode can be over 95%, leaving the transmitted light almost TM mode.

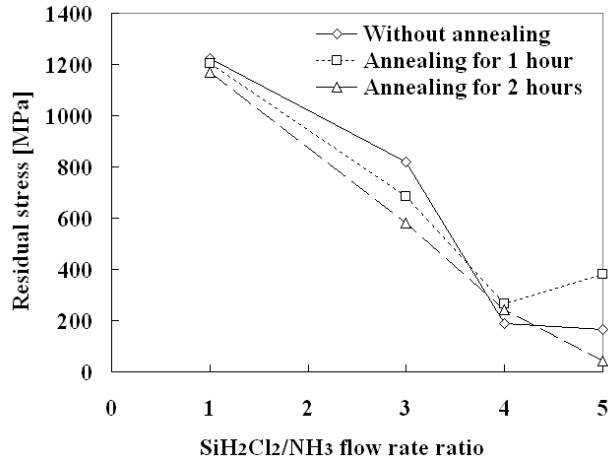
When combined with poly-silicon structures, a high-extinction-ratio pop-up micro PBS can be fabricated and easily integrated with other micro optical elements, such as a cylindrical lens to shape the incident beam, a grating to form tracking beams, a micro astigmatic lens to slightly alter the horizontal and vertical focal distances of the resulting spot on the photodiode array and mirrors as the reflectors, to form a micro optical pickup for short wavelength optical storage applications.

2. Silicon nitride film for 405 nm

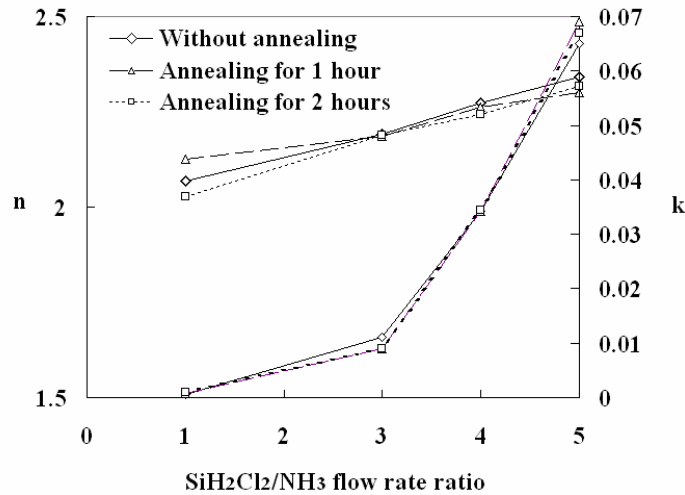
Silicon nitride can be deposited by the chemical vapor deposition with plasma enhancement (PECVD) or at low pressure (LPCVD). A stress-free PECVD silicon nitride film with high transparency at short wavelength can be obtained by a proper choice of process parameters, such as temperature and gas mixture, etc. [2] The most serious concern of PECVD silicon nitride is its poor chemical durability in HF solution, which is used to remove the sacrificial silicon dioxide layers [3]. The process results in high surface roughness and thickness variation, which will induce distorted wavefronts. As compared with PECVD silicon nitride, LPCVD silicon nitride has higher chemical durability against HF solution. To apply for short wavelength, LPCVD silicon nitride has to possess other two characteristics: lower stress to reduce curvature and lower absorption to enhance the optical utilization efficiency.

To reduce the thermal stress on silicon based materials, the LPCVD silicon nitride (SiN_x) can be silicon-rich by controlling the gas flow ratio, $\text{SiH}_2\text{Cl}_2:\text{NH}_3$, to be over 5. [4]. Our measurement shows that the transparency of LPCVD silicon-rich SiN_x is rather lower for its extinction coefficient k at 405 nm is as high as 0.07. According to Gardeniers' study [5], the mechanical and optical characteristics of the LPCVD SiN_x films are related to the following parameters, in decreasing order of importance: the gas flow ratio of Si and N containing precursors, temperature and pressure, etc. Since the silicon content is related to the high absorption at short wavelength, the effects of gas flow ratio and annealing condition on the

residual stress and optical transmission of SiN_x films were studied in our experiment. All SiN_x films were deposited by LPCVD at 850°C and 180 mTorr with various $\text{SiH}_2\text{Cl}_2/\text{NH}_3$ ratio (η) under constant total flow rate of 102 sccm. The deposited films were then annealed at 1050°C in nitrogen gas.



(a)



(b)

Fig. 1. Dependence of (a) residual stress and (b) complex refractive index, $n + ik$, on the reaction gas ratio for various annealing times.

The residual stress was measured after processing using a wafer curvature technique employing Stoney's equation. The dependence of the residual stress on the reaction gas ratio, η , for various annealing time is shown in Fig. 1(a). The film stress shows a general

decreasing trend with increasing SiH₂Cl₂/NH₃ ratio due to the increased silicon content. After annealing, the stress can be either increased or decreased by two competing mechanisms: the stress relaxation within the grain of the film and the film shrinkage due to dehydrogenation. [6]

The dependence of the complex refractive index, $n + ik$, on the reaction gas ratio for various annealing time is shown in Fig. 1(b). The n increases nearly linearly with increasing η while the k shows a sharp increase for $\eta > 3$, due to the increased content of silicon with high index and high absorption. For the SiN_x film to be used in the micro PBS, it should be low stress and low absorption. Since higher SiH₂Cl₂/NH₃ ratios decrease the stress but increase the absorption, a trade-off is required. Therefore, a SiH₂Cl₂/NH₃ ratio = 3 with two-hour annealing was selected to fabricate the lower stress (585 MPa) and lower absorption ($n = 2.189 + i0.0095$) micro PBS.

3. Optical design

The optical design of the SiN/Air/SiN stack is performed by using the characteristic matrix. Each layer is described by a 2×2 matrix, which relates to the components of the electric (or magnetic) field along the direction of propagation. The reflectivity, transmissivity and absorption of the stack can be derived from multiplication of the matrix of each layer together.

The characteristic matrix of the stack is given by [7]:

$$M = M_{SiN_1} M_{air} M_{SiN_2} = \begin{bmatrix} B \\ C \end{bmatrix} = \prod_{i=1}^3 \begin{bmatrix} \cos(\delta_i) & -\frac{i}{\eta_i} \sin(\delta_i) \\ -i\eta_i \sin(\delta_i) & \cos(\delta_i) \end{bmatrix} \begin{bmatrix} 1 \\ \eta_a \end{bmatrix}$$

where

$$\delta_i = \frac{2\pi}{\lambda} N_i d_i \cos(\theta_i)$$

δ_i is related to the complex refractive index N_i , the thickness d_i of the layers, wavelength λ , and the refraction angle θ_i as shown in Fig. 2. The optical admittances, η_i of the i -th layer and η_a of the air substrate are given by

$$\begin{aligned} \eta_i &= N_i \cos\theta_i && \text{for TE Mode} \\ \eta_a &= \cos\theta_a && \text{for TE Mode} \\ \eta_i &= N_i / \cos\theta_i && \text{for TM Mode} \\ \eta_a &= 1 / \cos\theta_a && \text{for TM Mode} \end{aligned} \quad (6)$$

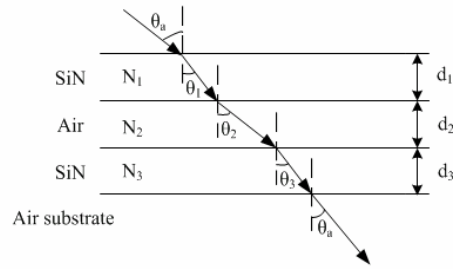


Fig. 2. Propagation of an electromagnetic wave through a stack of films of thickness d_i and refractive index N_i .

The reflectivity R , transmissivity T and absorption A of the incident light for both polarizations can be derived from Eqs. (1)~(6):

$$R = \left(\frac{\eta_a B - C}{\eta_a B + C} \right)^2, \quad T = \frac{4\eta_a R_e(\eta_a)}{(\eta_a B + C)(\eta_a B + C)^*}, \quad A = \frac{4\eta_a R_e(BC^* - \eta_a)}{(\eta_a B + C)^2} \quad (7)$$

If R_{TE} and T_{TE} are the reflectivity and transmissivity for the TE mode, and R_{TM} and T_{TM} for the TM mode, respectively, the optical characteristics of the micro PBS can be evaluated by two extinction ratios σ_T (for transmission) and σ_R (for reflection) defined as [1].

$$\sigma_T = 10 \times \log_{10} \left(\frac{T_{TM}}{T_{TE}} \right), \quad \sigma_R = 10 \times \log_{10} \left(\frac{R_{TE}}{R_{TM}} \right)$$

Our target is to have a PBS with extinction ratios for the transmitted light to be above 10, and for the reflected light to be above 20. From Eqs. (1) to (8), we calculated the optical performance of the stack at Brewster angle incidence as a function of d_1 , d_2 and d_3 , which are the thicknesses of the first silicon nitride layer, the air gap and the second silicon nitride layer, respectively. At Brewster angle incidence, the nominal reflectivity of the TM mode is zero. Therefore, to achieve high polarization extinction ratios, the reflectivity to transmissivity ratio of TE should be as high as possible. Besides, to reduce the fabrication complexity of the micro optical pickup, the thickness, d_1 , of the first silicon nitride layer is fixed to be 384 nm, which is the thickness of other micro optical elements. For example, the diffraction efficiency ratio of the 0th order beam and the ± 1 st order beams could be well controlled within 4~10 at this thickness for a micro-grating in the optical pickup using the three beam tracking method.

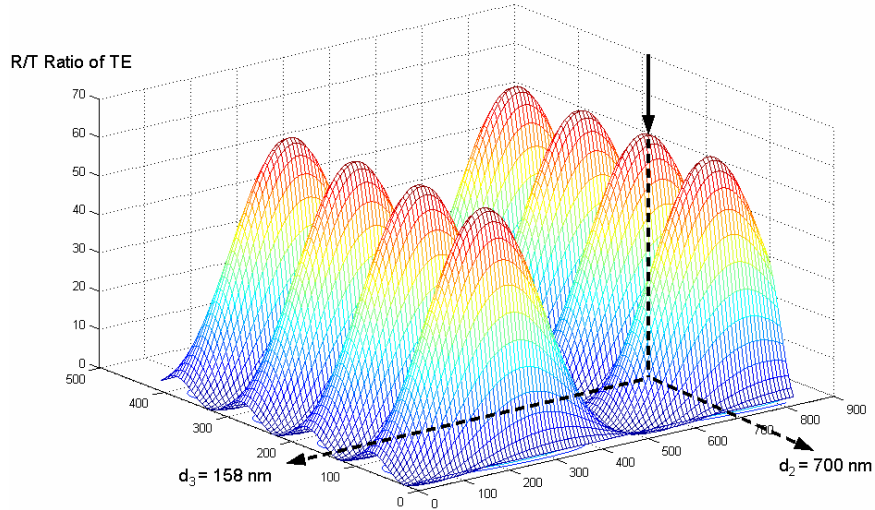


Fig. 3. Calculated reflectivity to transmissivity ratio of the TE mode as a function of d_2 and d_3 at the Brewster angle incidence.

As shown in Fig. 3, the reflectivity to transmissivity ratio of the TE mode can be over 50 around the points: $(d_2, d_3) = (210 \text{ nm}, 52 \text{ nm}), (210 \text{ nm}, 158 \text{ nm}), (210 \text{ nm}, 216 \text{ nm}), (210 \text{ nm}, 360 \text{ nm}), (700 \text{ nm}, 52 \text{ nm}), (700 \text{ nm}, 158 \text{ nm}), (700 \text{ nm}, 216 \text{ nm}),$ and $(700 \text{ nm}, 360 \text{ nm})$. If d_3 was selected to be 52 nm, the mechanical strength of the second silicon nitride film would be too low. On the contrary, if d_3 was selected to be thicker, the absorption for the transmitted light would increase.

Therefore, d_2 and d_3 were selected to be 700 nm to effectively minimize stiction and 158 nm to have adequate mechanical strength, respectively. The calculation also shows that $\sigma_T = 15 \pm 5$ and $\sigma_R = \text{infinity}$ can be achieved at $d_1 = 384 \pm 10 \text{ nm}, d_2 = 700 \pm 100 \text{ nm}$ and $d_3 = 152 \pm 30 \text{ nm}$. The process margin is also practical in current fabrication technology.

4. Structure design and device fabrication

The stack of two silicon nitride layers separated by an air gap can be fabricated by surface micromachining. The structure is shown in Fig. 4. A poly silicon capping ring is used to mount a stack of silicon dioxide and silicon nitride layers, which are deposited alternatively on the poly silicon frame. After HF solution releasing, the silicon dioxide layers are removed, leaving an air gap, whose height can be controlled by dimples.

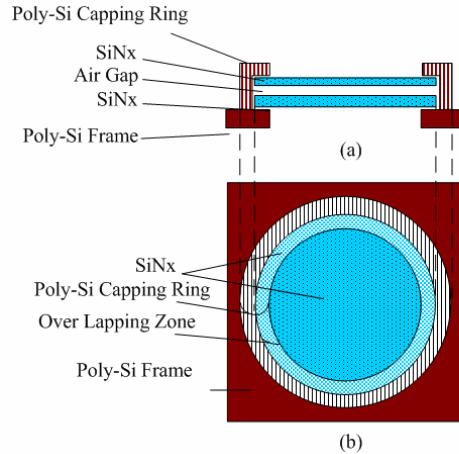


Fig. 4. Schematic drawing of the micro PBS: (a) cross-sectional and (b) top view.

The process to make a pop-up type micro PBS is illustrated in Fig. 5. The three-dimensional micro PBS consists of two layers of SiN_x optical film mounted in a poly-Si supporting frame. The support frame is held perpendicular to the substrate by locking with a micro-spring latch. To fabricate the device, a sacrificial silicon dioxide (SiO_2) layer was first deposited on the silicon substrate. Dimples and first anchors were then patterned in the sacrificial layer shown in Fig. 5(a). The first structural poly-Si was deposited by LPCVD and patterned to form a micro-frame. A SiO_2 layer and the first optical SiN_x layer were deposited and patterned. After depositing a SiO_2 layer, a 0.7- μm -deep dimple array was etched to control the air gap after releasing. The second optical SiN_x layer was deposited and patterned before depositing a SiO_2 layer. Both SiN_x layers were deposited aiming for a thickness slightly greater than the target value. The thickness was further reduced to the target value at the HF releasing step. After patterning anchors shown in Fig. 5(b), the second structural poly-Si layer was deposited and patterned to implement the micro-spring latches and the micro-frame shown in Fig. 5(c). The wafer was annealed for two hours at 1050°C in nitrogen to reduce the residual film stress. After releasing in HF solution, the micro PBS was then lifted to its vertical position by using a micro-probe shown in Fig. 5(d). The SEM micrographs of a pop-up micro PBS with a central aperture of 500 μm in diameter is shown in Fig. 6(a). Using the same process, the micro PBS was integrated with other components to form a micro optical pickup shown in Fig. 6(b).

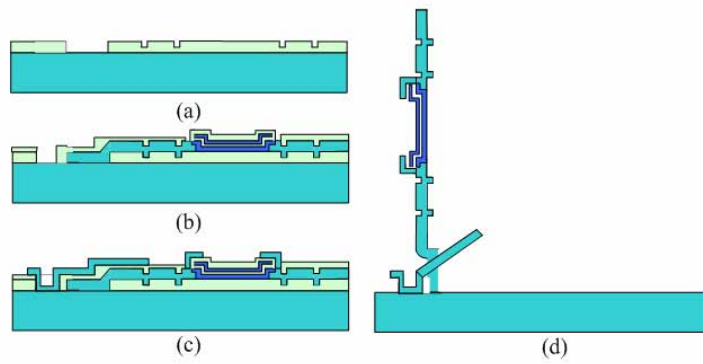
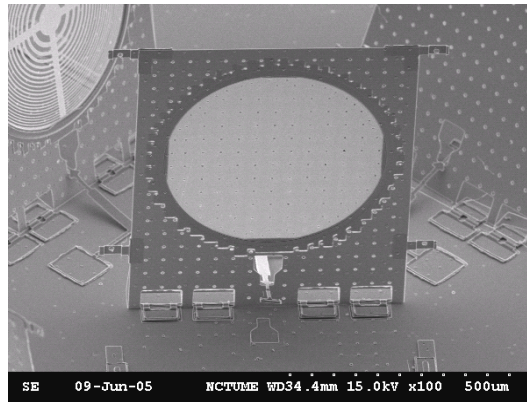
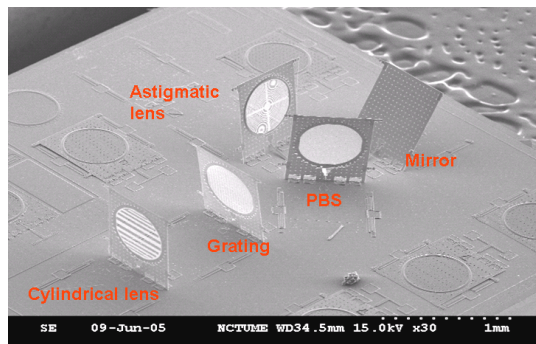


Fig. 5. Cross section of the processing sequence for fabricating the micro PBS.



(a)



(b)

Fig. 6. SEM photographs (a) the micro pop-up PBS and (b) a micro optical pickup.

5. Measurement and discussion

To measure the optical characteristic of the micro PBS, a GaN semiconductor laser at $\lambda=405$ nm was used as the light source. A retarder and a polarizer were used to adjust the polarization state of the light. An aperture of a diameter $200\ \mu\text{m}$ was used to yield the beam size comparable with the micro PBS at Brewster angle incidence. The beam profile was recorded on the CCD positioned at 10 mm from the micro PBS. The positions of maxima and minima are given in function of length converted from the pixel number on the CCD screen.

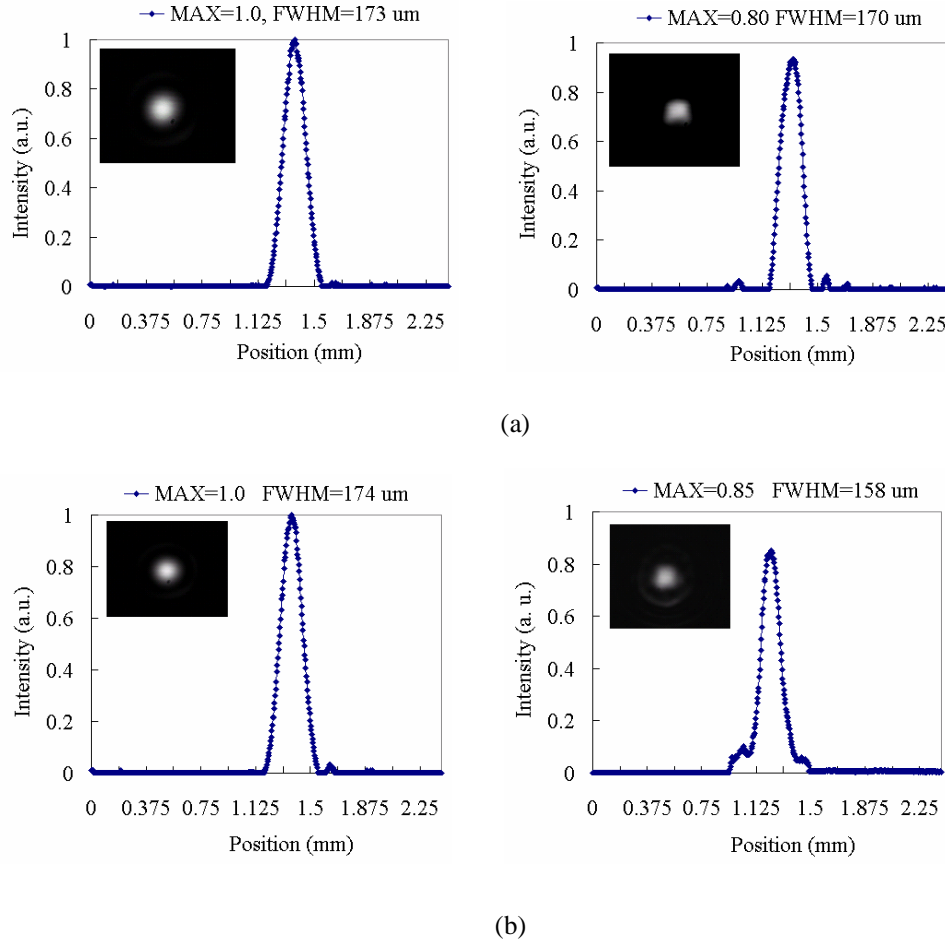


Fig. 7. (a) Beam profiles of TE mode before (left) and after (right) reflecting from the micro-PBS. (b) Beam profiles of TM mode before (left) and after (right) transmitting through the micro PBS.

The beam profiles of TE mode before and after reflecting from the micro-PBS are shown in Fig. 7(a). The peak reflectivity and transmissivity were measured to be 93% and 2.8 % of the incidence, respectively, while the absorption and scattering loss were 4.2% together. After reflection, the spot shape became changed obviously, which was caused by the stress-induced curvature of the micro PBS. The beam profiles of TM mode before and after transmitting through the micro-PBS are shown in Fig. 7(b). The peak reflectivity and

transmissivity were measured to be 0.3% and 85 % of the incidence, respectively, while the absorption and scattering loss were 14.7 % together. The measurement data are summarized in Table 1. $\sigma_T=15$ dB is close to the calculated value of 18, while the σ_R is as high as 25 dB. Both values match our design specification, $\sigma_T > 10$ and $\sigma_R > 20$, while the deviation was due to the scattering loss from the dimples, etch holes and surface roughness, 30 nm rms. A lower absorptive and lower stress silicon nitride can potentially yield a higher-extinction-ratio micro PBS using the similar processes for more demanding applications.

Table 1. Optical Performance of the Pop-up Micro PBS at Brewster Angle Incidence

	Calculation	Measurement
Reflectance of TE (%)	96	93
Transmittance of TE (%)	1.5	2.8
Reflectance of TM (%)	0	0.3
Transmittance of TM (%)	86	85
σ_T (dB)	18	15
σ_R (dB)	Infinite	25

6. Summary

A low stress silicon nitride film with low absorption at 405 nm was fabricated with the optimal process parameters. A stack that consists of two such silicon nitride layers separated by an air gap can function as a high polarization extinction-ratio PBS with $\sigma_T=15$, $\sigma_R=25$. The micro PBS can be integrated with other optical elements to form a micro optical bench for short wavelength optical storage applications.

Acknowledgments

The authors thank Prof. L. S. Huang, Institute of Applied Mechanics, NTU, for fruitful discussions. This work is supported by the Ministry of Economic Affairs under grant number 93-EC-17-A-07-S1-0011.